In-the-Field Calibration of All-Digital MIMO Arrays

Maryam Eslami Rasekh*, Bhagyashree Puranik†, Upamanyu Madhow‡, Mark Rodwell§

Dept. of Electrical and Computer Engineering
University of California Santa Barbara
Santa Barbara, California 93106
Email: {*rasekh, †bpuranik, ‡madhow, §rodwell}@ece.ucsb.edu

2022 IEEE Wireless Communications and Networking Conference (WCNC) | 978-1-6654-4266-4/22/$31.00 ©2022 IEEE | DOI: 10.1109/WCNC51071.2022.9771722

***Abstract*—A key goal of next generation networks is to scale hardware design and signal processing algorithms to mmWave and THz arrays with a large number of elements. Imperfect manufacturing and limitations of circuit design introduce variations in the gain and relative phase offset of transmit and receive array elements that must be compensated prior to beam formation for either communication or sensing. We propose a novel method for calibrating large arrays in the field by exploiting the sparsity of the spatial channel. While conventional calibration methods are susceptible to multipath components in the wireless channel, our approach is shown to be robust to multipath interference if the measurements are gathered from a sufficiently diverse set of locations.**

***Index Terms*—Array calibration, digital beamforming, massive MIMO, reciprocity, millimeter wave, THz**

I. Introduction

As emerging technologies look to millimeter wave (mmWave) and Terahertz (THz) frequencies for higher bandwidth and spatial reuse, massive MIMO architectures play a crucial role in realizing these gains. For sub-centimeter carrier wavelengths, hundreds, even thousands, of elements can be packed together on compact platforms, providing high beamforming gain, interference suppression, and, in the case of digitally controlled arrays, spatial multiplexing. In such a massive MIMO regime, it becomes particularly important to exploit regular array geometries and the spatial sparsity of mmWave/THz channels for efficient signal processing [1], [2]. However, in order to apply such models, we must develop techniques for calibrating amplitude and phase variations across the elements of the array. Manufacturing can be more challenging at small wavelengths, as small variations in RF circuitry and local oscillator distribution paths can cause large, unpredictable phase variations in the RF chain response of different array elements. At THz frequencies, even sub-millimeter path differences can produce large phase shifts, causing completely random phase offsets across the transmitter and receiver arrays. As a result, the spatial channels in uplink and downlink are effectively multiplied by different random vectors that must be estimated and compensated for in order to take advantage of channel sparsity and reciprocity (Fig. 1).

This work was supported in part by ComSenTer, one of six centers in JUMP, a Semiconductor Research Corporation (SRC) program sponsored by DARPA.

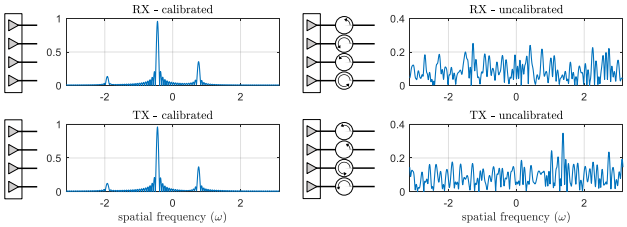

Fig. 1. Magnitude of spatial frequency domain representation of the channel with (left) and without (right) calibration. The channel seen by a calibrated array consists of a few spatial frequencies, corresponding to path directions, which are identical in uplink and downlink. Calibration offsets disrupt both frequency domain sparsity and path reciprocity of the channel.

Conventionally, array calibration is performed in a controlled environment (e.g., anechoic chamber where a pure single path channel is guaranteed) by exciting the array from a source in its boresight. In these conditions, the channel response is constant on the array antennas and the measured signal is the calibration vector itself. This procedure is costly and time consuming and its accuracy may be degraded by slight changes in calibration offsets over time, e.g., due to environmental effects or other sources of stress.

Contributions: We propose a framework for *post-deployment* uplink and downlink calibration of a base station array in an uncontrolled multipath environment, relying solely on the spatial sparsity of the channel. We begin with the observation that measurement of the array response from a *single* source through a pure line-of-sight (LOS) channel can be used to calibrate the array in a manner that suffices for beamforming. While such calibration is inaccurate if the signal is received through a multipath channel, we propose here a technique that synthesizes an "effective LoS source" using measurements from several sources (mobiles or nearby base stations) at different locations for joint calibration and spatial channel estimation. We exploit the location diversity across sources to mitigate distortion due to multipath via an "align and average" strategy, lining up the dominant paths of each source. We term the dominant path for a given source as its LOS path henceforth, since that is usually the scenario of interest, while noting that our approach also applies in scenarios with LOS blockage if there is a strong reflected path.

Our approach to isolating and lining up LOS paths is summarized as follows:

• Estimate pairwise spatial frequency differences between the LOS paths for different sources via sparse super-resolution techniques.

• Use these estimates to derotate and align measurements from different sources.

• Use the strongest singular vector of the aligned measurements as an "effective LOS measurement" for calibration.

• Optionally, reconstruct the multipath channel for each source via sparse estimation, and refine the estimated calibration vector from the original measurements conditioned on the reconstructed channels.

We observe that even strong multipath can be filtered out using measurements from as few as 10 sources using this technique, provided the measurements have sufficiently high SNR. We characterize the *per-element* SNR requirement, and discuss consequences for two-directional calibration (i.e., of both the transmit and receive arrays). In particular, we show that the use of geometric reciprocity can help relax SNR requirements for calibration in one direction by piggybacking on calibration in the reverse direction.

Related work: Calibration of RF chains has long been of interest, mainly for the goal of extending channel reciprocity to end-to-end uplink-downlink reciprocity. One approach used in the literature is to include dedicated hardware inside the RF circuitry for calibration. For instance, in [3], extra elements are added to the array that are not supported by a full RF chain and act as pilot transmitters for calibration. A more scalable and cost-efficient approach is to use external sources, either in controlled environments with a known channel response, as in [4], [5], or by jointly estimating the channel and calibration offsets. Without relying on the channel sparsity assumption, joint calibration and channel estimation requires many measurements and a high level of coordination between transmit and receive arrays [6]. In [7], the authors assume single path channels between the source and receiver and perform joint direction of arrival estimation and broadband calibration. Second order statistics are used in [8]–[10] to derive array offset parameters. These rely on a set of sources with single-path channels transmitting unknown but uncorrelated signals over time, utilizing the information in the observed covariance matrix for estimation of array gain and phase offsets, which are in turn used to estimate the AOA of each source. These techniques rely on rotational invariance of the source channels and therefore only apply to single path channels that excite only one spatial frequency on the array. In the presence of multipath, the performance of these methods is severely degraded, as we show in section V. With large enough bandwidth, multipath components can be separated in time, and the direction and delay of each path can be estimated jointly with array offsets. This approach is used in [11] for joint calibration and delay estimation using a wideband OFDM sequence. This method imposes a large bandwidth requirement on the procedure, and is susceptible to the existence of multipath components with close enough delays that can not be separated with the available bandwidth. Some studies have formulated the problem of blind calibration in the presence of multipath as a convex optimization problem. In [12], [13] the authors propose a semi-definite programming based convex optimization framework for joint estimation of sparse channels and calibration coefficients. These methods suffer from two major drawbacks. First, the assumption of on-grid sparsity for the channel model which is not accurate for a multipath channel with path directions dispersed *on a continuum*, and second, the computational complexity of these method for an array of length N is $\mathcal{O}(N^3)$ making it a poor match for massive MIMO arrays. In [14], a more efficient method is proposed for this task. However, it requires physical rotation of the target array to gather the necessary measurements, which may not be feasible post-deployment if antennas are mounted on a fixed platform. Here, we propose a scalable blind calibration algorithm that is robust to multipath, and therefore suitable for continuous in-the-field calibration.

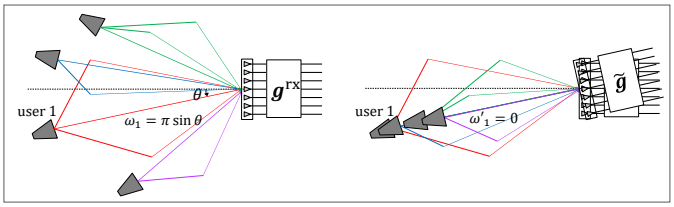

Fig. 2. Rotation of angular reference perception toward direction of user 1 and alignment of LOS components of channels with that of channel 1

II. System Model

The base station consists of separate, digitally-controlled transmit and receive arrays with N_{tx} and N_{rx} elements, respectively. For simplicity, we consider linear arrays with half-wavelength spacing, setting $N_{\mathrm{tx}} = N_{\mathrm{rx}} = N$. The nominal response vector for a unit-amplitude plane wave incident from angle θ is given by

$$\mathbf{r}(\omega) = \left[1, e^{j\omega}, e^{j2\omega}, \ldots, e^{j(N_{\mathrm{rx}}-1)\omega}\right]^T. \tag{1}$$

where $\omega = \pi \sin\theta$ is the *spatial frequency* corresponding to angle of arrival θ. Assuming that the transmit and receive arrays have identical orientation, a single-path channel excites the same spatial frequency in uplink and downlink, but with a constant phase shift due to the relative displacement of the arrays. This phase shift varies depending on the angle of incidence, meaning conventional channel reciprocity does not hold for *multipath* channels. However, *geometric* reciprocity still guarantees that the angles of departure and arrival are the same for *each path* in the channel. Thus, despite the absence of full channel reciprocity for displaced arrays, such *path reciprocity* can still be relied upon when beamforming toward the dominant path in the channel, provided the arrays are *calibrated*.

We denote the uplink (receiver) and downlink (transmitter) calibration vectors by $\mathbf{g}^{\mathrm{rx}}$ and $\mathbf{g}^{\mathrm{tx}}$, respectively. Our goal is to estimate these coefficients, up to a constant phase and

spatial frequency offset, via a simple training procedure. We first focus on receiver calibration, and later discuss how the framework can be applied to transmitter calibration.

The phase and amplitude of received signals are altered by the (multiplicative) receiver calibration vector,

$$\mathbf{g}^{\text{rx}}[n] = \alpha_n e^{j\phi_n}, \tag{2}$$

where $\alpha_n \in \mathbb{R}^+, \phi_n \in [0, 2\pi)$ and $\mathbf{v}[n]$ represents the scalar value of the n'th element of vector $\mathbf{v}$. Thus, a unit-amplitude single-path channel with angle of arrival θ (or spatial frequency ω) would result in the (noiseless) received signal vector

$$\mathbf{y}(\omega) = \text{diag}(\mathbf{g}^{\text{rx}})\mathbf{r}(\omega), \tag{3}$$

with $\mathbf{y}[n] = \mathbf{g}^{\text{rx}}[n]e^{jn\omega} = \alpha_n e^{j(n\omega+\phi_n)}, n = 0, ..., N_{\text{rx}} - 1$. If a channel measurement is taken inside an anechoic chamber using a source placed at $\theta = \omega = 0$, then a high SNR measurement would yield an accurate estimate of the calibration vector (up to a constant amplitude scaling and phase shift), since the channel is guaranteed to contain only the direct LOS path with a constant response across the array.

Calibrating with an LOS source from an unknown direction: If, on the other hand, the source is at an unknown direction θ_1 (spatial frequency ω_1), then the measurement is at a constant *frequency* offset away from the true calibration vector $\mathbf{g}^{\text{rx}}$. Interestingly, the offset vector, $\tilde{\mathbf{g}}^{\text{rx}}[n] = \alpha_n e^{j\phi_n + n\omega_1}$, is still a valid calibration vector as we can simply operate with a *shifted spatial frequency reference* by mapping any path direction ω to the shifted version $\tilde{\omega} = \omega - \omega_1$. This simply translates the channel response in spatial frequency, preserving sparsity. Furthermore, if both the transmitter and receiver are calibrated at the same (albeit unknown) offset direction, they share a common spatial frequency reference, so that geometric reciprocity is also preserved. Therefore, when pure LOS channel measurements are available to us, the calibration offsets can be (directly) measured up to a constant phase and spatial frequency offset, and channel sparsity and geometric reciprocity is attained.

Multipath model: In multipath channels, however, direct calibration is not possible. To recover the uplink calibration vector, we rely on a set of M channel measurements from users dispersed in the cell or other nearby base stations that take turns transmitting a predefined training sequence from different locations. Measurements are thereby separated in time domain and cross-user interference is avoided. Denoting the amplitude, direction, and spatial frequency of the LOS path for source m by a_m, θ_m and ω_m, respectively, the response vector corresponding to that path is $a_m\text{diag}(\mathbf{g}^{\text{rx}})\mathbf{r}(\omega_m)$, and the full multipath channel measurement is of the form

$$\begin{aligned}
\mathbf{y}_m &= \text{diag}(\mathbf{g}^{\text{rx}})\mathbf{h}_m + \boldsymbol{\nu}_m \\
&= a_m\text{diag}(\mathbf{g}^{\text{rx}})\mathbf{r}(\omega_m) && \leftarrow (\text{LOS}_m) \\
&+ \text{diag}(\mathbf{g}^{\text{rx}}) \sum_{k=1}^{K_m} a'_{m,k}\mathbf{r}(\omega'_{m,k}) && \leftarrow (\text{MP}_m) \\
&+ \boldsymbol{\nu}_m && \leftarrow (\text{noise})
\end{aligned} \tag{4}$$

where K_m is the number of multipath components in channel m, $a'_{m,k}$ and $\omega'_{m,k}$ are the complex amplitude and spatial frequency of the kth multipath component of source m, and $\boldsymbol{\nu}_m \sim \mathcal{CN}(\mathbf{0}, \sigma^2\mathbf{I})$ is the receiver noise vector. We use the notation MP_m as a shorthand for the total contribution of non line of sight (NLOS) multipath components, which is typically smaller than the LOS contribution. We treat this term as noise for our alignment of LOS paths across measurements for initial calibration, and then use sparse estimation techniques to estimate the multipath in order to refine our calibration.

Our measurement model (4) assumes *narrowband* signaling during calibration. Larger signaling bandwidths could be used to reject at least some of the multipath components, but we do not rely on that here, in order to demonstrate the generality of our approach.

III. Algorithm

In this section, we describe our algorithm for joint estimation of calibration coefficients and channels using measurements from M user locations. We first consider the uplink direction (receiver calibration) and then discuss how the framework is applied in the downlink for transmitter calibration.

Suppose that we take noise-free measurements from an LOS source at spatial frequency ω_1 as our calibration vector, as indicated in the previous section. This yields the effective calibration vector

$$\begin{aligned}
\tilde{\mathbf{g}}^{\text{rx}} &= \mathbf{y}_1 = a_1\text{diag}(\mathbf{g}^{\text{rx}})\mathbf{r}(\omega_1) \\
&= \left[a_1\alpha_n e^{j(\phi_1+n\omega_1)}\right]_{n=0:N_{\text{rx}}-1}.
\end{aligned} \tag{5}$$

which is shifted in spatial frequency by ω_1 while preserving sparsity and geometric reciprocity (see Fig. 2). We can therefore define

$$\begin{aligned}
\tilde{\alpha}_n &= |\mathbf{y}_1[n]| = |a_1|\alpha_n, \\
\tilde{\phi}_n &= \angle\mathbf{y}_1[n] = \phi_n + \angle a_1 + n\omega_1, \\
\tilde{\omega}_1 &= 0, \quad \tilde{a}_1 = 1.
\end{aligned}$$

in our shifted system.

Calibrating in multipath channels: In our proposed algorithm, we take the LOS response of the first measurement (ω_1, α_1) as our spatial frequency and phase reference. Using (5), we rewrite the channel measurement as

$$\mathbf{y}_1 = \tilde{\mathbf{g}}^{\text{rx}} + \tilde{\text{MP}}_1 + \boldsymbol{\nu}_1$$

where all the multipath components in the channel are frequency shifted according to the reference ω_1. A second measurement vector, $\mathbf{y}_2$, with LOS at (true) angle ω_2 is of the form

$$\mathbf{y}_2[n] = \tilde{\mathbf{g}}^{\text{rx}}[n]\frac{a_2}{a_1}e^{jn\tilde{\omega}_2} + \tilde{\text{MP}}_2 + \boldsymbol{\nu}_2$$

where $\tilde{\omega}_2 = \omega_2 - \omega_1$. Indeed, any new measurement can be transferred to the reference frame of $\tilde{\mathbf{g}}^{\text{rx}}$ by translating its LOS angle, ω_m, to our perceived coordinate system as $\tilde{\omega}_m = \omega_m - \omega_1$, and dividing its gain, a_m, by the gain of the first path to get $\tilde{a}_m = a_m/a_1$. The calibration procedure consists of translating this concept into an algorithm.

A. Estimating LOS frequencies in reference frame

For two noiseless LOS measurements, the frequency difference and gain ratio can be estimated from non-calibrated measurements $\mathbf{y}_m$ and $\mathbf{y}_1$ by forming the vector

$$\mathbf{z}_m[n] = \frac{\mathbf{y}_m[n]}{\mathbf{y}_1[n]} \approx \frac{a_m}{a_1} e^{jn(\omega_m - \omega_1)} = \tilde{a}_m e^{jn\tilde{\omega}_m} \tag{6}$$

and finding its peak in frequency domain. While (6) is a suitable way to construct $\mathbf{z}_m$ for noiseless and purely LOS channels, in a realistic environment it is better to first undo the amplitude scaling using a coarse absolute gain estimate, e.g., $\hat{\boldsymbol{\alpha}}_0[n] = \frac{1}{M}\sum_m |\mathbf{y}_m[n]|$, and then element-wise multiply $\mathbf{y}_m$ by the *conjugate* of $\mathbf{y}_1$ to produce

$$\mathbf{z}_m[n] = \frac{\mathbf{y}_m[n]\mathbf{y}_1^*[n]}{\hat{\boldsymbol{\alpha}}_0^2[n]}, \tag{7}$$

a mixture of frequencies, the strongest of which is the element-wise conjugate product of LOS components with frequency $\omega_m - \omega_1$. This dominant frequency can be accurately estimated using an off-grid sparse reconstruction algorithm such as Newtonized orthogonal matching pursuit (NOMP) [15], from the measurement model, $\mathbf{y}_m = \mathbf{A}\mathbf{z}_m$, where $\mathbf{A} = \mathbf{I}_N$, providing us with an estimate for $\tilde{\omega}_m = \omega_m - \omega_1$.

B. Aligning measurements

After estimating $\tilde{\omega}_m = \omega_m - \omega_1$ for all m, we align the (uncalibrated) LOS of all measurements with that of $\mathbf{y}_1$ by undoing this frequency offset as follows:

$$\begin{aligned}\tilde{\mathbf{y}}_m[n] &= \mathbf{y}_m[n]e^{-jn\tilde{\omega}_m} \\ &= a_m \mathbf{g}^{\text{rx}}[n]e^{j\omega_1 n} + \text{MP}_m[n]e^{jn\tilde{\omega}_m} + \boldsymbol{\nu}'_m[n] \\ &= \frac{a_m}{a_1}\tilde{\mathbf{g}}^{\text{rx}}[n] + \text{MP}'_m + \boldsymbol{\nu}'_m[n]. \end{aligned} \tag{8}$$

A geometric interpretation of this procedure is illustrated in Fig. 2. Note that these vectors are weighted copies of $\tilde{\mathbf{g}}^{\text{rx}}$ distorted by independent noise and multipath.

C. Averaging

In order to extract $\tilde{\mathbf{g}}^{\text{rx}}$, we form the $N_{\text{rx}} \times M$ matrix,

$$\mathbf{G} = [\tilde{\mathbf{y}}_1\ \tilde{\mathbf{y}}_2\ ...\ \tilde{\mathbf{y}}_M]\,. \tag{9}$$

We can now perform a singular value decomposition (SVD) on $\mathbf{G}$, and taking the strongest left singular vector

$$\hat{\mathbf{g}}^{\text{rx}} = \mathbf{u}_1(\mathbf{G}), \tag{10}$$

to obtain an estimate for the calibration vector $\tilde{\mathbf{g}}^{\text{rx}}$, shifted in spatial frequency by ω_1. Since the multipath distortions in different $\tilde{\mathbf{y}}$ vectors are independent while the LOS components are aligned, increasing the number of measurements M rapidly improves the accuracy of $\hat{\mathbf{g}}^{\text{rx}}$, as we demonstrate numerically in Section V.

D. Refinement via sparse channel reconstruction

We can further refine our estimate of $\tilde{\mathbf{g}}^{\text{rx}}$ by calibrating the original measurements with the output of (10) and obtaining estimates of the significant paths in each channel, $\{\tilde{a}_m, \tilde{\omega}_m, \tilde{a}_{m,k}, \tilde{\omega}_{m,k}\}$, via off-grid sparse estimation; we employ the Newtonized Orthogonal Matching Pursuit (NOMP [15] for this purpose. We then construct the full channel at each location as

$$\tilde{\mathbf{h}}_m = \tilde{a}_m \mathbf{r}(\tilde{\omega}_m) + \sum_{k=1}^{K_m} \tilde{a}_{m,k}\mathbf{r}(\tilde{\omega}_{m,k}) \tag{11}$$

and undo it in the original measurements to arrive at a new, more accurate set of vectors,

$$\tilde{\mathbf{y}}'_m[n] = \frac{\mathbf{y}_m[n]}{\tilde{\mathbf{h}}_m[n]}, \quad m \in \{1, ..., M\}. \tag{12}$$

We then form the refined matrix,

$$\mathbf{G}' = [\tilde{\mathbf{y}}'_1\ ...\ \tilde{\mathbf{y}}'_M] \tag{13}$$

and perform SVD to arrive at a refined estimate of $\tilde{\mathbf{g}}^{\text{rx}}$,

$$\hat{\mathbf{g}}^{\text{rx}} = \mathbf{u}_1(\mathbf{G}'). \tag{14}$$

Our numerical results show that this step can significantly reduce the calibration estimation error, provided the initial calibration vector estimate is sufficiently accurate.

Transmitter calibration: Downlink calibration is analogous to uplink, and the same procedure can be used to find $\tilde{\mathbf{g}}^{\text{tx}}$ from M measurements of the uncalibrated downlink channel. In order to obtain these measurements, the base station broadcasts orthogonal training sequences (e.g., baseband OFDM subcarriers) on its transmit array elements, and the users correlate the observed signals against each sequence to recover N_{tx}-dimensional measurement vectors, which are then fed back to the base station. We note that, for effective calibration, it is vital that both the transmitter and the receiver use *the same path of the same user* as their reference direction, so that $\tilde{\mathbf{g}}^{\text{tx}}$ and $\tilde{\mathbf{g}}^{\text{rx}}$ are consistent in their perceived orientation, and path reciprocity is upheld.

IV. Scaling and SNR requirement

While increasing the number of measurement locations improves estimation accuracy by averaging multipath and noise, the SNR of each measurement is a significant bottleneck in the success of the algorithm, specifically, the frequency difference estimation step of III-A. To quantify this bottleneck, consider two standard, unit-amplitude complex sinusoids, $\mathbf{x}_1[n] = e^{jn\omega_1}$ and $\mathbf{x}_2[n] = e^{jn\omega_2}$, of length N, distorted by complex Gaussian noise, $\boldsymbol{\nu}$, of variance σ^2. The per-entry SNR of each of these signals is $1/\sigma^2$. The frequency difference is found by multiplying the first vector by the conjugate of the second vector to obtain

$$\begin{aligned}\mathbf{z}[n] &= (\mathbf{x}_1[n] + \boldsymbol{\nu}_1[n])(\mathbf{x}_2[n] + \boldsymbol{\nu}_2[n])^* \\ &= \mathbf{x}_1[n]\mathbf{x}_2^*[n] + (\boldsymbol{\nu}_1[n]\mathbf{x}_2^*[n] \\ &\qquad + \boldsymbol{\nu}_2^*[n]\mathbf{x}_1[n]) + \boldsymbol{\nu}_1[n]\boldsymbol{\nu}_2^*[n] \\ &= e^{jn(\omega_1 - \omega_2)} + \boldsymbol{\nu}'[n] + \boldsymbol{\nu}''[n] \end{aligned} \tag{15}$$

where $\mathbb{E}[(\boldsymbol{\nu}'[n])^2] = 2\sigma^2$ and $\mathbb{E}[(\boldsymbol{\nu}''[n])^2] = \sigma^4$. Thus the per-entry SNR of vector $\mathbf{z}$ is $1/\sigma_z^2 = 1/(2\sigma^2 + \sigma^4)$. If the input SNR is low (e.g., less than 0 dB), the σ^4 term becomes dominant and the SNR of our frequency difference measurement diminishes drastically. The per-element SNR is therefore a bottleneck that cannot be offset simply by increasing the number of measurement sources M, because correct estimation of the relative channels is crucial for aligning the measurements. Hence, this low SNR regime should be avoided and per-element SNR must be above a threshold for every measurement source that we use.

In MIMO communication, the link budget is typically designed for beamformed communication, ensuring *beamformed* SNR is kept at an adequate, relatively constant level. Consequently, the *per-element* SNR decreases by a factor of $1/N$ as array size N grows large. Therefore, in a practical setting, each calibration measurement must be aggregated over a number of symbols proportional to array size to provide sufficient per-element SNR for frequency difference estimation. The measurement complexity of this scheme is therefore $\mathcal{O}(N)$.

Piggybacking: Due to geometric reciprocity, the LOS spatial frequencies, $\{\tilde{\omega}_m = \omega_m - \omega_1\}$, estimated in the process of calibrating one direction can be reused when calibrating the opposite direction. Indeed, having precomputed estimates for the LOS frequencies allows bypassing of the initial frequency difference estimation step, which is the most SNR-sensitive step. As shown in our results, this can reduce the SNR requirement for the calibration procedure by a factor of N. In principle, piggybacking can be done in either direction: downlink calibration may use frequency estimates obtained during uplink calibration or vice versa.

Computational complexity: The most computationally intensive steps in the proposed algorithm are the sparse channel (or dominant frequency) estimation step and the SVD calculation. For the former, we use the NOMP algorithm which has complexity $\mathcal{O}(N \log N)$, while the complexity of SVD is $\mathcal{O}(MN)$. The overall computational complexity of our scheme is therefore $\mathcal{O}(N \log N + MN)$. Since the algorithm requires a relatively small number of measurement sources M, the computational burden scales near linearly with array size. In comparison, the benchmark approach of [12] has a complexity of $\mathcal{O}(LN^2)$ where L is the length of the observation sequence used to estimate the covariance matrix of the channel response.

V. Numerical Results

In this section we evaluate the performance of our approach via Monte Carlo simulations. Results are averaged over 100 realizations for each setting. We assume the LOS of all user channels have the same magnitude and model the multipath as one or more paths (specified for each case) with randomly chosen spatial frequencies maintaining a minimum separation of $4\pi/N$ from that of the LOS. Calibration phases and amplitudes are generated uniformly at random over $(0, 2\pi)$ and $(0.8, 1.2)$, respectively. As a benchmark, we consider the algorithm of [8] for sensor calibration which relies on second order channel statistics derived from measurement of simultaneous yet independent source transmissions over a long interval. We set the number of sources to 20 and assume the interval is long enough (infinite) to measure the channel covariance exactly. This algorithm assumes single-path channels from all sources and its performance is degraded significantly with even small multipath in the channels. We also report the performance of the standard calibration procedure that assumes measurements from a single source with no multipath (i.e., in an anechoic chamber). We assume noiseless reception for both of these benchmark procedures.

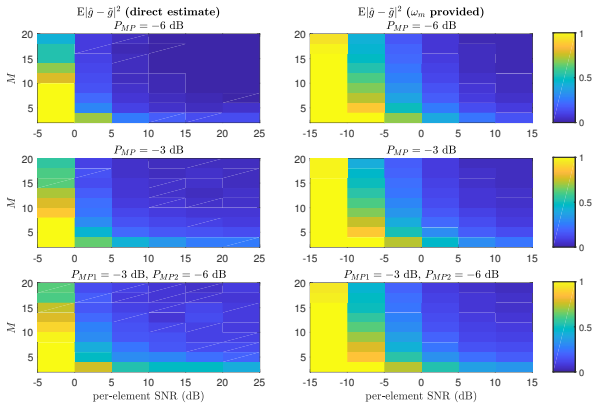

Fig. 3. Performance as a function of aggregate per-element SNR and number of measurement locations with different levels of multipath (strengths reported relative to LOS); left: standalone estimate, right: piggybacked estimate.

In Fig. 3 we report the mean squared error of calibration estimates obtained using our approach as a function of per-element SNR and number of measurement locations, M, for a 100-element receiver with different levels of multipath. It should be noted that these graphs are identical for uplink and downlink calibration assuming the same measurement sequence length and identical transmit power and receiver sensitivity for the user device and base station antenna elements. In this case, the orthogonal sequence transmission and correlation can be abstracted as an identity transform, and there is no meaningful difference between applying the algorithm in uplink and downlink. The results reported in Fig. 3 demonstrate that, with high enough measurement SNR, the algorithm is able to overcome significant multipath with even a small number of measurement locations. We also clearly see the per-element SNR bottleneck described in section IV; at per-element SNR of below 5 dB - corresponding to 25 dB beamformed SNR which is sufficiently high for beamformed communication - the algorithm fails regardless of the number of measurement locations. In the right-hand column graphs, we have plotted the same heatmaps for the case where the initial spatial frequency estimates are supplied from high SNR readings in the opposite direction. In this case, the SNR requirement is significantly lower which confirms our prediction that this first step of estimating the relative LOS spatial frequency offsets is the SNR bottleneck of the algorithm.

Fig. 4 depicts the (noiseless) performance of our algorithm, with and without the refinement step and with different number

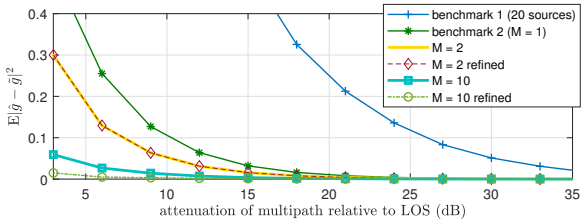

Fig. 4. Performance of proposed algorithm and benchmarks as a function of multipath strength (assuming one NLOS multipath component in the channel).

of measurement locations, against that of the benchmark algorithms. This figure demonstrates clearly the strength of our proposed approach in accurate calibration of arrays in the presence of even the strongest levels of multipath. We also observe that the refinement step can boost performance significantly at high M, yet for $M = 2$ there is virtually no gain from refinement. The reason behind this dynamic is that when taking SVD of only 2 measurements, the multipath is not rejected effectively and multipath frequencies seep into our initial estimate, $\hat{\mathbf{g}}$, and consequently cause parasitic frequencies in the sparse reconstructed channel estimate. Without an accurate channel estimate, the refinement step does not improve calibration accuracy, and may even degrade it.

VI. Conclusions

We presented a technique for post-deployment calibration of MIMO base station transceivers over noisy multipath channels. By aggregating measurements from a diverse set of locations in the cell, the algorithm is able to average out the independent multipath components and emulate a pure LOS channel to measure uplink and downlink calibration offsets. The calibration estimates can further be refined via sparse reconstruction of the full multipath channels that are in turn used to recover more accurate copies of the calibration vector from the raw measurements.

Our simulations demonstrated the robustness of the proposed approach against strong multipath components in the channel, which makes it suitable for on-the-fly calibration in realistic deployment environments. We found that the performance of this algorithm is sensitive to noise power on each antenna element, and therefore the training sequence used for measuring the channel of each source must be long enough to aggregate sufficient per-element SNR. For a typical beamformed communication budget, this length scales linearly with the number of elements in the array, as demonstrated by our numerical results. We also showed, however, that the path reciprocity available to spatially displaced transmitter and receiver arrays can be leveraged to relax this SNR requirement for one of the arrays by piggybacking on the high accuracy channel estimates obtained in the other.

While we have developed our calibration framework for channel models corresponding to ideal RF and mixed signal processing, in practice, nonlinearities in the signal path, such as ADC quantization, amplifier saturation, and dynamic range, must be accounted for. A detailed treatment of such effects, alongside experimental verification of the proposed framework, is left for future work.

References

[1] Ramina Ghods, Alexandra Gallyas-Sanhueza, Seyed Hadi Mirfarshbafan, and Christoph Studer, "BEACHES: Beamspace channel estimation for multi-antenna mmWave systems and beyond," in *2019 IEEE 20th International Workshop on Signal Processing Advances in Wireless Communications (SPAWC)*. IEEE, 2019, pp. 1–5.

[2] Mohammed Abdelghany, Upamanyu Madhow, and Antti Tölli, "Beamspace Local LMMSE: An Efficient Digital Backend for mmWave Massive MIMO," in *2019 IEEE 20th International Workshop on Signal Processing Advances in Wireless Communications (SPAWC)*. IEEE, 2019, pp. 1–5.

[3] Ashok Agrawal and Allan Jablon, "A calibration technique for active phased array antennas," in *IEEE International Symposium on Phased Array Systems and Technology, 2003.* IEEE, 2003, pp. 223–228.

[4] Boon Chong Ng and Chong Meng Samson See, "Sensor-array calibration using a maximum-likelihood approach," *IEEE Transactions on Antennas and Propagation*, vol. 44, no. 6, pp. 827–835, 1996.

[5] Guizhou Wu, Min Zhang, and Fucheng Guo, "On the use of a calibration emitter for direct position determination with single moving array in the presence of sensor gain and phase errors," *Digital Signal Processing*, p. 102734, 2020.

[6] Haralabos Papadopoulos, Ozgun Y Bursalioglu, and Giuseppe Caire, "Avalanche: Fast RF calibration of massive arrays," in *2014 IEEE Global Conference on Signal and Information Processing (GlobalSIP)*. IEEE, 2014, pp. 607–611.

[7] Krishnaprasad Nambur Ramamohan, Sundeep Prabhakar Chepuri, Daniel Fernández Comesaña, and Geert Leus, "Blind sensor array calibration and DOA estimation of broadband sources," in *2019 53rd Asilomar Conference on Signals, Systems, and Computers*. IEEE, 2019, pp. 1304–1308.

[8] Arogyaswami Paulraj and Thomas Kailath, "Direction of arrival estimation by eigenstructure methods with unknown sensor gain and phase," in *ICASSP'85. IEEE International Conference on Acoustics, Speech, and Signal Processing*. IEEE, 1985, vol. 10, pp. 640–643.

[9] Richard Roy and Thomas Kailath, "ESPRIT-estimation of signal parameters via rotational invariance techniques," *IEEE Transactions on acoustics, speech, and signal processing*, vol. 37, no. 7, pp. 984–995, 1989.

[10] Yonina C Eldar, Wenjing Liao, and Sui Tang, "Sensor calibration for off-the-grid spectral estimation," *Applied and Computational Harmonic Analysis*, vol. 48, no. 2, pp. 570–598, 2020.

[11] Tarik Kazaz, Mario Coutino, Gerard JM Janssen, and Alle-Jan van der Veen, "Joint blind calibration and time-delay estimation for multiband ranging," in *ICASSP 2020-2020 IEEE International Conference on Acoustics, Speech and Signal Processing (ICASSP)*. IEEE, 2020, pp. 4846–4850.

[12] Çağdaş Bilen, Gilles Puy, Rémi Gribonval, and Laurent Daudet, "Convex optimization approaches for blind sensor calibration using sparsity," *IEEE Transactions on Signal Processing*, vol. 62, no. 18, pp. 4847–4856, 2014.

[13] Rémi Gribonval, Gilles Chardon, and Laurent Daudet, "Blind calibration for compressed sensing by convex optimization," in *2012 IEEE International Conference on Acoustics, Speech and Signal Processing (ICASSP)*. IEEE, 2012, pp. 2713–2716.

[14] Amir Leshem and Mati Wax, "Array calibration in the presence of multipath," *IEEE Transactions on Signal Processing*, vol. 48, no. 1, pp. 53–59, 2000.

[15] Babak Mamandipoor, Dinesh Ramasamy, and Upamanyu Madhow, "Newtonized orthogonal matching pursuit: Frequency estimation over the continuum," *IEEE Transactions on Signal Processing*, vol. 64, no. 19, pp. 5066–5081, 2016.